

Enantioselective Hydroboration of Ketones Catalyzed by Rare-Earth-Metal Complexes Supported with Phenoxy-Functionalized TsDPEN Ligands

Qishun Yu, Chengrong Lu,* and Bei Zhao*

Cite This: *Organometallics* 2021, 40, 2529–2537

Read Online

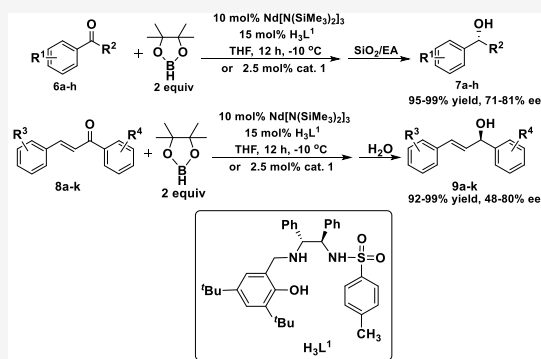
ACCESS |

Metrics & More

Article Recommendations

Supporting Information

ABSTRACT: Six novel chiral rare-earth-metal complexes bearing the phenoxy-functionalized TsDPEN ligand H_3L^1 ($H_3L^1 = N-((1R,2R)-2-((3,5\text{-di-}i\text{-tert-butyl-2-hydroxybenzyl)amino)-1,2\text{-diphenylethyl})-4\text{-methylbenzenesulfonamide}$) were synthesized successfully and well characterized. The solid-state structures of four tetranuclear rare-earth-metal complexes $[RE_2L^1_3]_2$ (RE = Nd (1), Sm (2), Eu (3), Gd (4)) and the dual-core yttrium complex $Y_2L^1_3$ (5) were determined by X-ray diffraction, respectively. The structure of lanthanum complex 6 was speculated by the 1H DOSY spectroscopy in THF- d_8 together with DFT calculations. Complexes 1–5 were employed to catalyze the enantioselective hydroboration of ketones and α,β -unsaturated ketones using pinacolborane (HBpin) as a reductant, and complex 1 gave better outcomes in comparison to the others. The corresponding secondary alcohols were obtained in excellent yields and moderate ee values. The same results were also achieved using the combined catalyst system of the neodymium amide $Nd[N(SiMe_3)_2]_3$ with the phenoxy-functionalized TsDPEN ligand H_3L^1 in a 1:1.5 molar ratio.



INTRODUCTION

Metal-catalyzed enantioselective reactions are some of the important practical strategies for the synthesis of chiral compounds. The enantioselectivities mainly depend on the chiral ligands; thus, the design of chiral ligands is of great importance. *N*-(*p*-Tosyl)-1,2-diphenylethylene-1,2-diamine, simplified as TsDPEN (Figure 1a), and its derivatives have

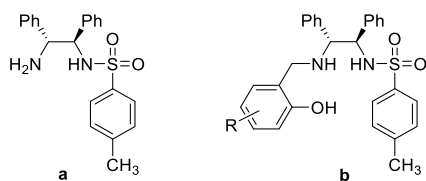


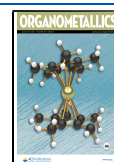
Figure 1. TsDPEN and phenoxy-functionalized TsDPEN.

proved to be excellent ligands and were used in asymmetric transfer hydrogenations catalyzed by Ru or Rh complexes,¹ Michael addition reactions catalyzed by Ru or Co complexes,² and Mannich reactions catalyzed by Ni complexes.³ Epoxidation⁴ and alkynylation⁵ were catalyzed by $FeCl_3 \cdot 6H_2O$ or $VOSO_4$ and CuI combined with TsDPEN in an *in situ* catalysis manner, respectively. In the above cases, the catalyst loading was relatively low, from 0.1 to 10 mol %, the yields of the target molecules were good to excellent (33–100%), and the enantioselectivities were good to excellent (42–99%).

In order to enhance the enantioselectivities of the catalysts, one efficient strategy—phenoxy-functionalized chiral ligands—was introduced in the design of ligands. In the past decade, phenoxy-functionalized prolinolates were developed to improve the chiral induction of prolinols in a variety of the asymmetric reactions by our group. Many systems of rare-earth-metal complexes bearing chiral phenoxy-functionalized prolinolates were synthesized and well characterized and were employed in asymmetric Michael additions,⁶ epoxidations,⁷ hydroborations,⁸ and hydrophosphonylations,⁹ respectively. It is noted that only one case of chiral phenoxy-functionalized TsDPEN ligands (Figure 1b) was employed in the preparation of chiral silicon Lewis acid catalysts, which were used in asymmetric Diels–Alder cycloadditions.¹⁰ If the prolinolates we used are replaced by the above TsDPEN subunit, what kind of rare-earth-metal complexes will we get and will the enantioselectivities of the desired complexes be improved in the asymmetric catalytic reactions? In order to find the answer, the modification of phenoxy-functionalized TsDPEN ligands,

Received: May 4, 2021

Published: July 9, 2021



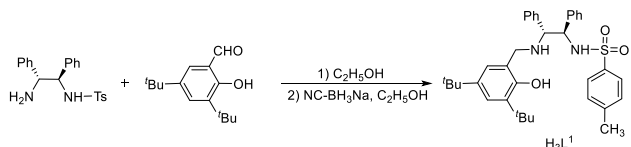
followed by the preparation of the corresponding rare-earth-metal complexes, and tests of their effectiveness in enantioselective transformation were carried out.

Enantioselective hydroboration is a common, efficient, and safe method to produce optically enantiopure secondary alcohols from ketones. Metal-based catalytic enantioselective hydroborations of ketones were developed using Co complexes bearing iminopyridine oxazoline ligands,¹¹ Mn complexes bearing bis(oxazolylmethylidene)-isoindoline pincer ligands,¹² Ni complexes bearing oxazoline ligands,¹³ or Mg¹⁴ and Al¹⁵ complexes bearing BINOLs as the catalytic system; meanwhile RE-based complexes combined with *N,N'*-dioxide ligands,¹⁶ phenoxy-functionalized prolinolates,⁸ or Trost ligands¹⁷ were also employed in the transformation. Though enantioselective hydroboration is a reaction that has attracted much attention, highly efficient systems are still rare and need to be constantly developed, because the target enantiopure secondary alcohols are key organic synthesis intermediates.¹⁸ Thus, some rare-earth-metal complexes supported with phenoxy-functionalized TsDPEN ligands were prepared and their catalytic behavior for enantioselective hydroboration of ketones was investigated. Herein we report these results.

RESULTS AND DISCUSSION

With the commercially available chiral TsDPEN in hand, the phenoxy-functionalized TsDPEN ligand H_3L^1 (*N*-((1*R*,2*R*)-2-((3,5-di-*tert*-butyl-2-hydroxybenzyl)amino)-1,2-diphenylethyl)-4-methylbenzenesulfonamide) was prepared according to a previous work.¹⁹ The reaction is shown in Scheme 1.

Scheme 1. Synthesis of H_3L^1



Occasionally, the crystal structure was characterized by X-ray diffraction, shown in Figure 2. The chiralities of the two chiral centers C8 and C15 are both the *R* configuration, indicating that the ligand did not racemize during the phenoxy functionalization.

Reactions of the rare-earth-metal amides $RE[N(SiMe_3)_2]_3$ ($RE = Nd$ (1), Sm (2), Eu (3), Gd (4), Y (5)) with H_3L^1 in a 1:1.5 molar ratio in THF gave the final products in high yields (Scheme 2). Crystals of complexes 1–4 suitable for X-ray diffraction were obtained from a hexane/toluene mixed solvent at room temperature, and four chiral tetranuclear rare-earth-

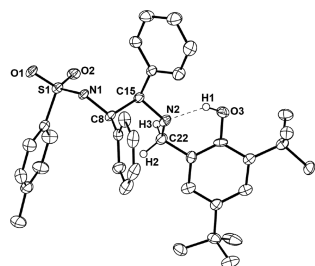
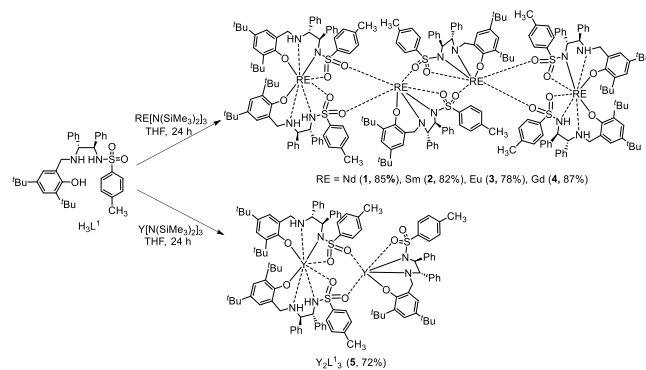


Figure 2. ORTEP diagram of the structure of the chiral ligand H_3L^1 . Thermal ellipsoids are drawn at the 50% probability level. Hydrogen atoms, except those on C22 and O3 atoms, are omitted for clarity.

Scheme 2. Synthesis of Complexes 1–5



metal complexes $[RE_2L^1_3]_2$ ($RE = Nd$ (1), Sm (2), Eu (3), Gd (4)) were characterized and determined. Since complexes 1–4 are isostructural, only the representative molecular structure of complex 1 is depicted in Figure 3. Details of the crystallographic data of crystals 1–4 are summarized in Table S1, and the corresponding selected bond lengths and angles are provided in Tables S2–S5.

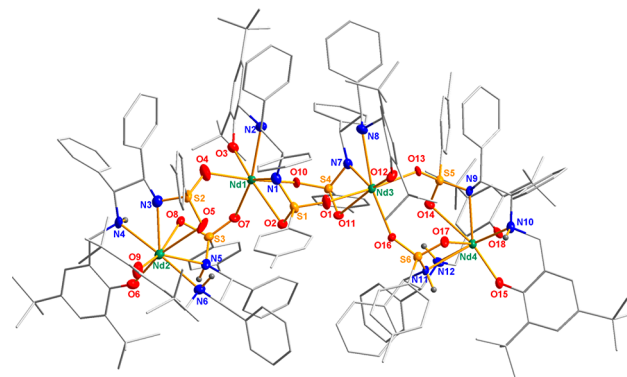


Figure 3. Molecular structure of complex 1. Aromatic substituents are shown in the form of wireframes, whereas the other atoms are shown by thermal ellipsoids drawn at the 50% probability level. Hydrogen atoms, except those on the N4–N6 and N10–N12 atoms, are omitted for clarity.

Complexes 1–4 are complicated monoclinic systems and have tetranuclear structures bearing six ligands. As shown in Figure 3, the solid-state structure of 1 is a dimer, linked by the oxygen atoms from sulfonyl groups. The geometric configurations around Nd1 and Nd3 are the same, as are those of Nd2 and Nd4. Only the coordination environments of Nd1 and Nd2 are discussed in detail. The central metal Nd1 has a 7-coordinated structure and a twisted-decahedral configuration, where O4 and O10 atoms occupy the two vertices with a O4–Nd1–O10 bond angle of 174.0°, slightly deviating from the ideal 180°; meanwhile N1, N2, O3, O7, and O2 atoms form the equatorial plane, since the sum of the bond angles 361.9° (N(1)–Nd(1)–N(2) 62.9(2)°, N(2)–Nd(1)–O(3) 74.2(2)°, O(3)–Nd(1)–O(7) 87.3(2)°, O(7)–Nd(1)–O(2) 83.4(2)°, O(2)–Nd(1)–N1 54.1(2)°) are close to the ideal 360°. The Nd1–N1 and Nd1–N2 bond lengths are 2.462(7) and 2.660(7) Å, respectively. The Nd1– μ -O2 (sulfonyl oxygen) bond length is 2.681(6) Å, much longer than 2.190(6) Å for Nd1–O3 (aryloxo), a type of σ bond. Other Nd1– μ -O bond lengths, such as the distances from Nd1 to

bridging oxygen atoms O4, O7, and O10, are 2.404(6), 2.415(6), and 2.421(5) Å, respectively. This indicates that the interactions between Nd1 and the three oxygen atoms from three sulfonyl groups are similar.

The central metal Nd2 has an 8-coordinated structure and a twisted-octahedral configuration. The approximate equatorial plane is comprised by the two aryl oxygen atoms O6 and O9 and the two sulfonyl oxygen atoms O5 and O8, since the sum of the bond angles around Nd2 is 362.8° (O(6)–Nd(2)–O(9) 91.3(3)°, O(9)–Nd(2)–O(5) 92.3(3)°, O(5)–Nd(2)–O(8) 83.6(2)°, O(8)–Nd(2)–O(6) 95.6(2)°), close to the ideal 360°. The two vertex N4 and N6 atoms are located on the both sides of the equatorial plane, with a bond angle of 176.9(2)°, close to the ideal 180°. The Nd2–N3, Nd2–N4, Nd2–N5, and Nd2–N6 bond lengths are 2.494(8), 2.615(7), 2.466(7), and 2.679(7) Å, respectively. The average Nd2–O (aryloxo) bond length is 2.207 Å, while the average Nd2– μ -O (sulfonyl oxygen) bond length is 2.720 Å.

The bond parameters in complexes 2–4 are similar to the corresponding values in complex 1, when the differences in ionic radii are taken into account.

The solid-state structure of complex 5 is shown in Figure 4, and it was proved to be a dual-core structure bearing three

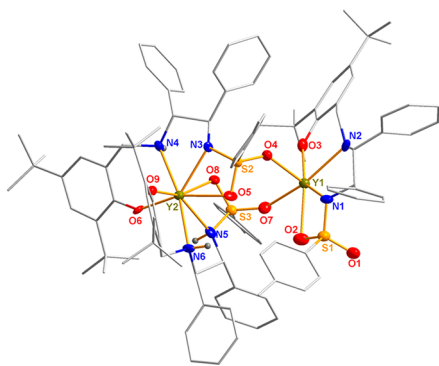


Figure 4. Molecular structure of complex 5. Aromatic substituents are in the form of wireframes, whereas the other atoms are shown by thermal ellipsoids drawn at the 50% probability level. Hydrogen atoms, except those on the N4–N6 atoms, and the coordinated solvents toluene and DCM are omitted for clarity.

ligands: that is, Y_2L_3 is the simplified formula. Details of the crystallographic data of crystal 5 are summarized in Table S1, and selected bond lengths and angles are provided in Table S6. The coordination environments of Y1 and Y2 atoms are similar to those of the corresponding Nd1 and Nd2 atoms in complex 1. The central metal Y1 has a 6-coordinated structure and a pentagonal configuration, where an O4 atom occupies the vertex and N1, N2, O3, O7, and O2 atoms form the equatorial plane, since the sum of the bond angles 362.8° is close to the ideal 360° (N(1)–Y(1)–N(2) 66.9(3)°, N(2)–Y(1)–O(3) 76.4(3)°, O(3)–Y(1)–O(7) 89.4(3)°, O(7)–Y(1)–O(2) 72.5(3)°, O(2)–Y(1)–N(1) 57.6(3)°). The Y1–N1 and Y1–N2 bond lengths are 2.350(9) and 2.527(9) Å, respectively. The Y1– μ -O2 (sulfonyl oxygen) bond length is 2.516(8) Å, much longer than 2.135(7) Å for Y1–O3 (aryloxo). Other Y1– μ -O bond lengths, such as the distances from Y1 to bridging oxygen atoms O4 and O7, are 2.289(7) and 2.281(7) Å, respectively.

The central metal Y2 has an 8-coordinated structure and a twisted-octahedral configuration. The approximate equatorial

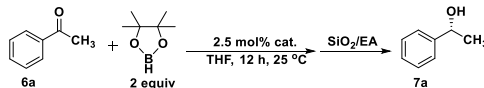
plane is comprised by the two aryl oxygen atoms O6 and O9 and the two sulfonyl oxygen atoms O5 and O8, since the sum of the bond angles around Y2 is 365.8° (O(6)–Y(2)–O(9) 91.7(3)°, O(9)–Y(2)–O(5) 90.9(2)°, O(5)–Y(2)–O(8) 85.8(2)°, O(8)–Y(2)–O(6) 97.4(3)°). The two vertices are N4 and N6 atoms, with a bond angle of 169.0(3)°, deviating from the ideal 180°. The Y2–N3, Y2–N4, Y2–N5, and Y2–N6 bond lengths are 2.479(8), 2.500(8), 2.418(9), and 2.580(8) Å, respectively. The average Y2–O (aryloxo) bond length is 2.158 Å, while the average Y2– μ -O (sulfonyl oxygen) bond length is 2.587 Å.

When the differences in ionic radii between Nd(III) and Y(III) are taken into account, the different aggregation structures of complexes 1 and 5 are reasonable and acceptable. The more open environment around neodymium may be more conducive to the coordination and dissociation process of the substrate and is beneficial for the reactivities.

In order to gain a deeper insight into the aggregation in solution, the structure of complex 5 in THF was confirmed by a ^1H DOSY NMR analysis. The ^1H DOSY spectrum (Figure S14; diffusion coefficient D_t determined as $4.50 \times 10^{-10} \text{ m}^2/\text{s}$) shows that the hydrodynamic radius (r_h) of complex 5 in THF- d_8 is 10.4 ± 0.5 Å (calculated by the Stocks–Einstein equation), which is comparable to the corresponding value r_{av} of 9.9 ± 0.5 Å calculated from crystal 5 according to a known method.²⁰ It reveals that complex 5 has the same dual-core structure whether it is in THF or in the solid state.

Using the same metathesis reaction, complex 6 was prepared by the treatment of $\text{La}[\text{N}(\text{SiMe}_3)_2]_3$ with H_3L^1 in a 1:1.5 molar ratio in THF. However, crystals suitable for an X-ray diffraction analysis were not available. To clarify the possible structure of complex 6, a diffusion coefficient D_t determination of powder 6 in THF- d_8 was conducted. The ^1H DOSY spectrum (Figure S15; diffusion coefficient D_t determined as $4.26 \times 10^{-10} \text{ m}^2/\text{s}$) shows that the hydrodynamic radius (r_h) of complex 6 in THF- d_8 is 11.0 ± 0.6 Å (calculated by the Stocks–Einstein equation). When we replaced the Y atom of the dual-core structure 5 by an La atom, the structure could be optimized using Gaussian16 at the B3PW91/6-31G** level (MWB46 for La)²¹ and the corresponding value (r_{av}) was calculated as 9.9 ± 0.5 Å, while when the Sm atom of tetranuclear structure 2 was replaced by an La atom, the corresponding value (r'_{av}) of 14.4 ± 0.7 Å was obtained. According to the above calculations, the hydrodynamic radius of complex 6 (11.0 Å) is relatively closer to the average radius (9.9 Å) when 6 is assumed to be a dinuclear molecule; thus, complex 6 in THF is speculated to exist as a dual-core complex.

To investigate the catalytic behavior of the chiral complexes 1–5, enantioselective hydroboration of acetophenone 6a was carried out as a model reaction. Fortunately, using HBpin as a reducing agent, we could get the chiral 1-phenyl-1-ethanol 7a quantifiably in THF with ee values varying from 18 to 57% for 12 h at room temperature (Table 1, entries 2–6). Obviously, the enantioselectivities of 7a decreased when the central rare-earth-metal atom radii of complexes 1–5 decreased, and the catalyst Nd-1 performed well. No better enantioselectivities of 7a were obtained after screening of additives (Table S7) and solvents (Table S10). A deliberate addition of 30 mol % of $\text{HN}(\text{SiMe}_3)_2$ in the catalytic system of Nd-based complex 1 was carried out, which was a test to simulate the *in situ* catalyst system. A comparable moderate ee value (60%) was observed, and meanwhile the excellent yield of 7a was maintained (Table

Table 1. Enantioselective Hydroboration of Acetophenone Catalyzed by Complexes 1–5^a


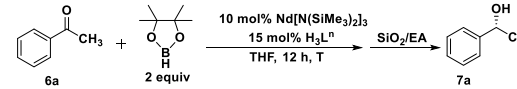
entry	cat.	additive	yield ^b (%)	ee ^c (%)
1			trace	nd
2	Nd-1		>99	57
3	Sm-2		>99	43
4	Eu-3		>99	40
5	Gd-4		>99	37
6 ^d	Y-5		>99	18
7 ^e	Nd-1	HN(SiMe ₃) ₂	>99	60
8 ^f	Nd[N(SiMe ₃) ₂] ₃ /H ₃ L ¹		>99	60
9 ^f	La[N(SiMe ₃) ₂] ₃ /H ₃ L ¹		>99	35

^aReaction conditions unless specified otherwise: **6a** (0.3 mmol), THF (2 mL). ^bHPLC yield. ^cDetermined by chiral HPLC. ^dThe amount of Y-5 was 5 mol %. ^eThe amount of HN(SiMe₃)₂ was 30 mol %. ^fLn[N(SiMe₃)₂]₃ 10 mol %, H₃L¹ 15 mol %.

1, entries 7 and 8). This indicates that complex **1** is likely to be the real catalytic species in the reaction and the existence of HN(SiMe₃)₂ has no negative effect on the transformation. Therefore, the following investigation was carried out in an *in situ* catalysis manner. The enantioselective hydroboration in the presence of an *in situ* La-based system was then checked; however, a disappointing outcome was obtained (Table 1, entry 9). Thus, the Nd-based catalytic combination is the optimal choice for the model reaction.

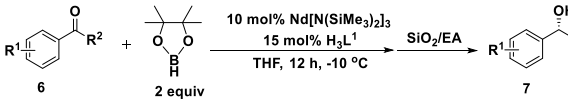
In general, variation of the temperature has an obvious effect on the enantioselectivities. After screening, the ee value of **7a** increased to 73% at −10 °C. However, further cooling to −20 °C was deleterious to the enantioselectivities (Table 2, entries 1–3). In view of the important role of chiral ligands in the enantioselectivities, a series of phenoxy-functionalized TsDPEN ligands H₃L²–H₃L¹² were prepared and tested subsequently.²⁰ Disappointingly, the aforementioned proligand H₃L¹ remains the best choice in the current transformation (Table 2, entries 4–14). To make sure of the effectiveness of the phenoxy-functionalized strategy, a study of chiral TsDPEN was carried out as well and the ee value was as low as 15% (Table 2, entry 15). The chiral ligand H₃L¹³ with the more rigid bridge (*R,R*)-cyclohexanediamino was synthesized and employed in the transformation. The ee value of **7a** decreased to 38% (Scheme S3), while on replacement with ligand H₃L¹, the ee value was 73% under the same conditions (Table 2, entry 2). Hence, the enantioselective hydroboration of acetophenone occurred smoothly for 12 h at −10 °C in the presence of 10 mol % of the precatalyst Nd[N(SiMe₃)₂]₃ with 15 mol % of the phenoxy-functionalized TsDPEN ligand H₃L¹.

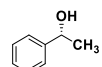
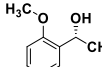
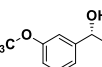
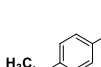
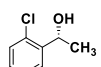
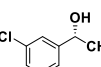
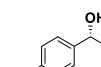
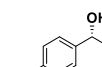
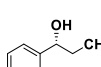
A variety of substituted ketones were investigated under the optimal conditions. The results are summarized in Table 3. Substrates with both electron-donating and electron-withdrawing groups on the phenyl rings gave the corresponding alcohol in high yields, varying from 95% to 99%. The location of the substituents has a slight effect on the enantioselectivities of the target alcohols. The substrates bearing *ortho*-position substituents gave comparably good ee values, while the ee values of the *para*-substituted substrates decreased, such as **7b** versus **7d** and **7e** versus **7g**. Meanwhile, substrates with electron-donating substituents gave slightly better ee values. When the substrate was not a methyl ketone, such as

Table 2. Screening of the Ligands and Temperature of Enantioselective Hydroboration of Acetophenone Catalyzed by Nd[N(SiMe₃)₂]₃^a


entry	ligand	T (°C)	yield ^b (%)	ee ^c (%)
1	H ₃ L ¹	0	>99	62
2	H ₃ L ¹	−10	>99	73
3	H ₃ L ¹	−20	>99	71
4	H ₃ L ²	−10	>99	69
5	H ₃ L ³	−10	>99	55
6	H ₃ L ⁴	−10	>99	37
7	H ₃ L ⁵	−10	>99	39
8	H ₃ L ⁶	−10	>99	42
9	H ₃ L ⁷	−10	>99	47
10	H ₃ L ⁸	−10	>99	−35
11	H ₃ L ⁹	−10	>99	−60
12	H ₃ L ¹⁰	−10	>99	−54
13	H ₃ L ¹¹	−10	>99	38
14	H ₃ L ¹²	−10	>99	45
15	TsDPEN	−10	>99	15

^aReaction conditions: **6a** (0.3 mmol), THF (2 mL), 12 h. ^bHPLC yield. ^cDetermined by chiral HPLC.

Table 3. Enantioselective Hydroboration of Ketones Catalyzed by Nd[N(SiMe₃)₂]₃ Combined with H₃L¹^{a–c}


 7a yield: 99% ee: 73%	 7b yield: 99% ee: 82%	 7c yield: 98% ee: 81%
 7d yield: 99% ee: 74%	 7e yield: 96% ee: 81%	 7f yield: 97% ee: 70%
 7g yield: 95% ee: 68%	 7h yield: 98% ee: 65%	 7i yield: 99% ee: 71%

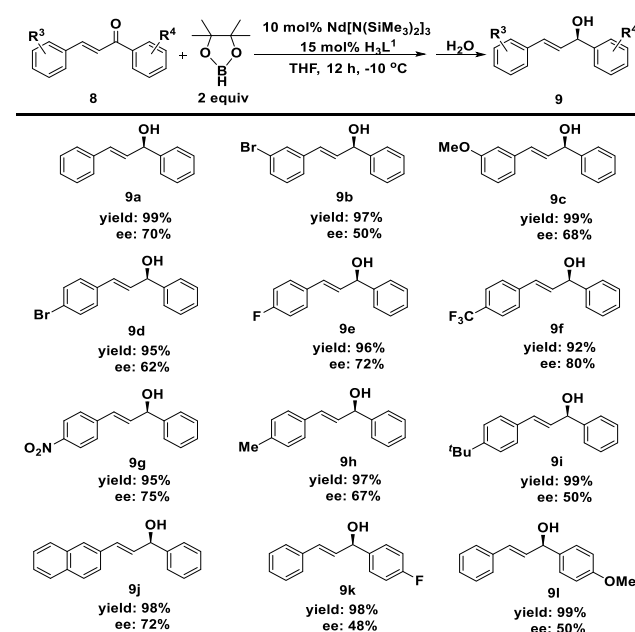
^aReaction conditions: **6** (0.3 mmol), Nd[N(SiMe₃)₂]₃ (0.03 mmol), H₃L¹ (0.045 mmol), THF (2 mL). ^bIsolated yield. ^cDetermined by chiral HPLC.

propiophenone **6i**, the enantioselective hydroboration also occurred quantitatively with a comparable ee value of 71%.

In comparison with that of simple ketones, enantioselective hydroboration of α,β -unsaturated ketones is more challenging, which is generally complicated by competitive 1,2- and 1,4-reduction processes. Enantioselective reduction of substituted

α,β -unsaturated ketones was investigated with the reductant HBpin in the current system, and Table 4 recorded the results.

Table 4. Enantioselective Hydroboration of α,β -Unsaturated Ketones Catalyzed by $\text{Nd}[\text{N}(\text{SiMe}_3)_2]_3$ Combined with H_3L^1 ^{a-c}

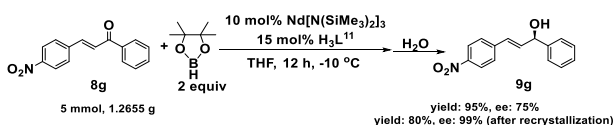


^aReaction conditions: **8** (0.3 mmol), $\text{Nd}[\text{N}(\text{SiMe}_3)_2]_3$ (0.03 mmol), H_3L^1 (0.045 mmol), THF (2 mL). ^bIsolated yield. ^cDetermined by chiral HPLC.

A good tolerance of the various substituents was observed. Excellent yields for the allylic alcohols **9a–l** were obtained, while the ee values varied significantly (48–80%). When R^3 was a strongly electron withdrawing group, such as a trifluoromethyl or nitro group, the ee values of the corresponding allylic alcohols were improved (Table 4, **9e–g**). However, when R^4 was either an electron-donating group, such as a methoxy group, or an electron-withdrawing group, such as fluorine, the ee values were worse (Table 4, **9k, l**). In comparison with previous works, the outcomes for enantioselective reduction of substituted α,β -unsaturated ketones using current chiral rare-earth-metal catalysts are much better than those of rare-earth-metal-based catalyst bearing Trost ligands (1 example; the ee value was 30%)¹⁷ but slightly inferior to those of functionalized prolinolates (12 examples; ee values varied from 77% to 89%).⁸ Furthermore, as shown in Scheme 3, the hydroboration of α,β -unsaturated ketones on a gram scale proceeded smoothly with a satisfactory yield and high enantioselectivity.

Subsequently, the absolute configurations of the secondary alcohol series **7** and **9** were determined by HPLC spectra and optical rotation on comparison with our previous work.^{8,17}

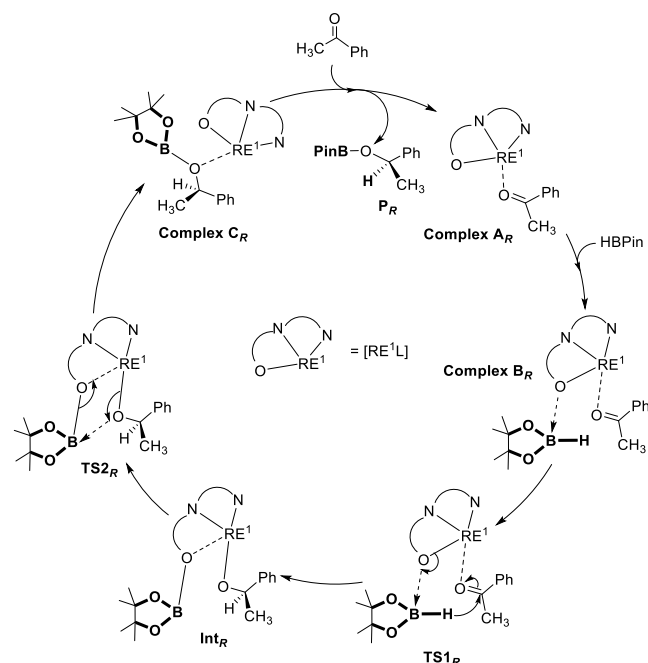
Scheme 3. Amplification Reaction of the Preparation of Compound 9g



According to the ^1H DOSY experiments of complexes **5** and **6**, the complexes are likely to be dinuclear in THF. In combination with the DFT calculations, it is seen that the relatively open space around RE^1 is conducive to the coordination of the substrate. Thus, it is possible that RE^1 plays a catalytic role, while RE^2 and the surrounding ligands stabilize the entire complex. Thus, catalysts are simplified as $[\text{RE}^1\text{L}]$, while the second half containing RE^2 is omitted for clarity.

On the basis of a proposed mechanism,¹⁷ a similar mechanism was suggested and is depicted in Scheme 4.

Scheme 4. Possible Mechanism of Enantioselective Hydroboration of Ketones Catalyzed by $[\text{RE}^1\text{L}]$



Initially, the substrate ketone **6a** coordinates to the rare-earth metal to give the complex A_R , followed by the coordination of the reducing agent HBpin with the alkoxy oxygen via a boron atom to generate the complex B_R . Hydride migration to a carbonyl carbon takes place to produce Int_R through TS1_R , and then σ -bond metathesis of O-B and O-RE^1 occurs to yield complex C_R via the tetracyclic TS2_R . Finally, the dissociation of the desired borate P_R occurs in concert with the regeneration of catalyst **I**.

CONCLUSION

In conclusion, four chiral tetranuclear rare-earth-metal complexes $[\text{RE}_2\text{L}^1_3]_2$ ($\text{RE} = \text{Nd}$ (**1**), Sm (**2**), Eu (**3**), Gd (**4**)) and a dual-core yttrium complex Y_2L^1_3 (**5**) were prepared and were well characterized by X-ray diffraction. The La-based complex **6** was also synthesized in the same way, and the structure was speculated by ^1H DOSY spectroscopy in $\text{THF-}d_8$ and DFT calculations. The catalytic reactivities of complexes **1–5** in the enantioselective hydroboration of ketones were investigated using HBpin as the reductant. Finally, the catalytic system has optimal conditions for the enantioselective reduction of simple ketones of 10 mol % of $\text{Nd}[\text{N}(\text{SiMe}_3)_2]_3$ combined with 15 mol % of H_3L^1 in THF for 12 h at $-10\text{ }^\circ\text{C}$. The desired chiral alcohols with excellent yields (95–99%) and moderate ee values (65–82%) were obtained. Further-

more, the more challenging enantioselective hydroboration of α,β -unsaturated ketones was carried out with the current catalytic system, which gave us the corresponding chiral allylic alcohols with excellent yields (92–99%) and moderate ee values (48–80%) as well.

EXPERIMENTAL SECTION

General Procedures. All reagents were commercially available (reagent grade) and were used as received unless otherwise noted. Experiments involving air- and moisture-sensitive components were performed in a glovebox or using the standard Schlenk techniques with freshly distilled solvents. Solvents, such as tetrahydrofuran, toluene, and hexane, were degassed and distilled from sodium benzophenone ketyl before use. Various readily available ketones were distilled after treatment with calcium hydride. Flash chromatography was performed using 200/300 mesh silica gel with freshly distilled solvents with a SepaBean machine. Different types of commercial silica flash columns were used and equilibrated with the appropriate solvent system prior to use. Carbon, hydrogen, and nitrogen analyses were performed by direct combustion with a Thermo Scientific Flash Smart Elemental Analyzer instrument. IR spectra were recorded with a VERTEX 70⁺ HYPERION 2000 instrument. Nuclear magnetic resonance spectra were obtained on a Bruker 400/500 MHz spectrometer (CDCl₃, C₆D₆, and THF-*d*₈ were used as solvents). Chemical shifts for NMR spectra are reported in units of parts per million (ppm) downfield from SiMe₄ (0.0) and are relative to the signal of the deuterated solvent. Multiplicities are given as s (singlet), d (doublet), t (triplet), q (quartet), dd (doublets of doublets), or m (multiplets). High-resolution mass spectra were obtained using a Bruker ESI-TOF instrument. HPLC analysis was performed with a SHIMADZU LC-20AD instrument equipped with a quaternary pump, employing a Daicel Chiralcel column at 35 °C. Optical rotation was measured using a SGW-2 Polarimeter equipped with a sodium vapor lamp at 589 nm.

General Procedure for the Preparation of Complexes 1–6. To a THF (10 mL) solution of the proligand H₃L¹ (0.8764 g, 1.5 mmol) was slowly added a THF solution of RE[N(SiMe₃)₂]₃ (1 mmol). The mixture was stirred at room temperature for 12 h. After THF was removed under vacuum, the solid residue was washed with hexane to remove HN(SiMe₃)₂. Crystals were obtained at room temperature from a mixed solvent of hexane and THF.

Characteristic data of complex [Nd₂L¹]₂ (1): light blue crystal, 0.86 g, yield 85%; IR (cm⁻¹) ν 2949.5, 2360.4, 1472.7, 1440.2, 1413.2, 1359.9, 1182.7, 1110.1, 931.0, 909.6, 806.5, 742.7, 697.6, 666.7. Anal. Calcd for C₂₁₆H₂₅₂Nd₂N₁₂O₁₈S₆: C, 63.68; H, 6.24; N, 4.13. Found: C, 63.24; H, 6.23; N, 3.93.

Characteristic data of complex [Sm₂L¹]₂ (2): colorless crystal, 0.84 g, yield 82%; IR (cm⁻¹) ν 2950.9, 2342.1, 1599.8, 1473.3, 1440.5, 1359.7, 1189.8, 1110.4, 1048.3, 934.2, 910.7, 806.9, 698.2, 666.3. Anal. Calcd for C₂₁₆H₂₅₂Sm₂N₁₂O₁₈S₆: C, 63.30; H, 6.20; N, 4.10. Found: C, 62.82; H, 6.33; N, 3.96.

Characteristic data of complex [Eu₂L¹]₂ (3): maroon crystal, 0.80 g, yield 78%; IR (cm⁻¹) ν 2950.1, 2361.8, 1598.5, 1441.0, 1360.0, 1189.3, 1110.5, 1049.6, 1016.0, 933.2, 873.5, 807.5, 698.5, 666.5. Anal. Calcd for C₂₁₆H₂₅₂Eu₂N₁₂O₁₈S₆·4Tol: C, 65.52; H, 6.40; N, 3.76. Found: C, 65.22; H, 6.64; N, 4.15.

Characteristic data of complex [Gd₂L¹]₂ (4): colorless crystal, 0.90 g, yield 87%; IR (cm⁻¹) ν 2949.4, 2364.7, 1599.7, 1472.0, 1440.0, 1359.5, 1161.6, 1110.3, 1047.3, 1016.1, 931.1, 806.5, 697.3, 666.4. Anal. Calcd for C₂₁₆H₂₅₂Gd₂N₁₂O₁₈S₆·Tol: C, 63.50; H, 6.21; N, 3.98. Found: C, 63.15; H, 6.75; N, 3.98.

Characteristic data of complex Y₂L¹ (5): colorless crystal, 0.69 g, yield 72%; ¹H NMR (400 MHz, THF-*d*₈) δ 7.41 (s, 2H), 7.23 (s, 3H), 7.07 (s, 2H), 6.96 (s, 15H), 6.86 (s, 2H), 6.75 (d, *J* = 25.9 Hz, 11H), 6.60 (s, 7H), 6.50 (s, 1H), 6.45 (s, 5H), 6.35 (s, 3H), 5.14 (s, 1H), 5.02 (s, 1H), 4.69 (s, 1H), 4.21 (s, 1H), 4.00 (s, 2H), 3.31 (s, 2H), 3.00 (s, 2H), 2.92–2.72 (m, 2H), 2.62 (s, 1H), 2.22 (s, 3H), 1.63 (s, 12H), 1.34 (d, *J* = 15.6 Hz, 4H), 1.30 (s, 8H), 1.25 (s, 2H), 1.19 (s, 5H), 1.04 (d, *J* = 19.8 Hz, 30H); IR (cm⁻¹) ν 2950.5, 2360.7,

1558.4, 1488.5, 1441.5, 1396.6, 1360.5, 1196.3, 1112.9, 1056.4, 936.6, 809.1, 698.9, 668.8. Anal. Calcd for C₁₀₈H₁₂₆Y₂N₆O₉S₃·Tol·2DCM: C, 64.22; H, 6.36; N, 3.84. Found: C, 63.94; H, 6.46; N, 4.14.

Characteristic data of complex 6: colorless crystal, 0.75 g, yield 74%; ¹H NMR (400 MHz, THF-*d*₈) δ 7.16 (d, *J* = 2.5 Hz, 3H), 6.97 (d, *J* = 6.7 Hz, 9H), 6.88–6.79 (m, 6H), 6.67 (d, *J* = 6.5 Hz, 3H), 6.62–6.47 (m, 24H), 6.38 (d, *J* = 2.5 Hz, 3H), 4.48 (d, *J* = 10.6 Hz, 3H), 4.03–3.88 (m, 6H), 3.11 (d, *J* = 10.7 Hz, 3H), 2.61 (s, 3H), 2.09 (s, 9H), 1.52 (s, 27H), 1.12 (s, 27H); IR (cm⁻¹) ν 2955.7, 2361.9, 1473.1, 1445.9, 1411.2, 1293.8, 1264.3, 1144.1, 1116.6, 1066.8, 931.3, 805.3, 696.9, 671.5. Anal. Calcd for C₁₀₈H₁₂₆La₂N₆O₉S₃: C, 64.02; H, 6.27; N, 4.15. Found: C, 63.97; H, 6.35; N, 4.12.

General Procedure for the Hydroboration Reaction of Ketones. RE[N(SiMe₃)₂]₃ (0.03 mmol) was added to a solution of H₃L¹ (0.045 mmol) in THF (1 mL). The reaction mixture was stirred at room temperature for 15 min. HBpin (0.6 mmol) was added in one portion, and the mixture was stirred at –10 °C for an additional 15 min before the corresponding ketone (0.3 mmol) in 1 mL of THF was added. After it was stirred for 12 h at –10 °C, the reaction mixture was quenched with SiO₂ (1 g) and the solvent was evaporated. The residue was purified by flash column chromatography on silica gel to afford the pure chiral alcohol. The enantiomeric excess of the alcohol was determined by an HPLC analysis on a chiral stationary phase.

Characteristic Data of Secondary Alcohols 7. (R)-1-Phenylethan-1-ol (7a):¹⁷ colorless oil, 36.3 mg, yield 99%; [α]_D²⁰ = +33.60 (*c* = 0.21 in CHCl₃); ¹H NMR (400 MHz, CDCl₃) δ 7.45–7.30 (m, 1H), 7.28–7.13 (m, 4H), 4.82 (d, *J* = 6.4 Hz, 1H), 1.82 (s, 1H), 1.42 (d, *J* = 6.5 Hz, 3H); ¹³C NMR (101 MHz, CDCl₃) δ 144.8, 127.5, 126.5, 124.4, 69.4, 24.1; 73% ee, HPLC Daicel column OD-H, 98% hexanes, 2% ^tPrOH, 1.0 mL/min, 10.4 min (major), 11.5 min (minor); HRMS (ESI-MS) *m/z* [M + Na]⁺ calcd for C₈H₁₀ONa 145.0624, found 145.0632.

(R)-1-(2-Methoxyphenyl)ethan-1-ol (7b):¹⁷ colorless oil, 45.0 mg, yield 99%; [α]_D²⁰ = +23.54 (*c* = 0.23 in CHCl₃); ¹H NMR (400 MHz, CDCl₃) δ 7.34 (dd, *J* = 7.5, 0.9 Hz, 1H), 7.28–7.20 (m, 1H), 6.96 (t, *J* = 7.5 Hz, 1H), 6.88 (d, *J* = 8.2 Hz, 1H), 5.09 (q, *J* = 6.5 Hz, 1H), 3.86 (s, 3H), 2.66 (s, 1H), 1.51 (d, *J* = 6.5 Hz, 3H); ¹³C NMR (101 MHz, CDCl₃) δ 156.6, 133.4, 128.3, 126.1, 120.8, 110.5, 66.6, 55.3, 22.9; 82% ee, HPLC Daicel column OD-H, 98% hexanes, 2% ^tPrOH, 1.0 mL/min, 8.4 min (minor), 10.1 min (major); HRMS (ESI-MS) *m/z* [M + Na]⁺ calcd for C₉H₁₂O₂Na 175.0730, found 175.0728.

(R)-1-(3-Methoxyphenyl)ethan-1-ol (7c):¹⁷ colorless oil, 44.8 mg, yield 98%; [α]_D²⁰ = +34.28 (*c* = 0.24 in CHCl₃); ¹H NMR (400 MHz, CDCl₃) δ 7.26 (t, *J* = 8.1 Hz, 1H), 6.94 (d, *J* = 5.6 Hz, 2H), 6.84–6.78 (m, 1H), 4.86 (d, *J* = 6.4 Hz, 1H), 3.81 (s, 3H), 1.99 (d, *J* = 11.2 Hz, 1H), 1.48 (d, *J* = 6.5 Hz, 3H); ¹³C NMR (101 MHz, CDCl₃) δ 159.8, 147.6, 129.6, 117.7, 112.9, 110.9, 70.4, 55.2, 25.1; 81% ee, HPLC Daicel column OD-H, 98% hexanes, 2% ^tPrOH, 1.0 mL/min, 12.1 min (major), 13.4 min (minor); HRMS (ESI-MS) *m/z* [M + Na]⁺ calcd for C₉H₁₂O₂Na 175.0730, found 175.0730.

(R)-1-(4-Methoxyphenyl)ethan-1-ol (7d):¹⁷ colorless oil, 45.0 mg, yield 99%; [α]_D²⁰ = +52.42 (*c* = 0.18 in CHCl₃); ¹H NMR (400 MHz, CDCl₃) δ 7.32–7.22 (m, 2H), 6.91–6.82 (m, 2H), 4.77 (d, *J* = 6.4 Hz, 1H), 3.77 (s, 3H), 3.29 (s, 1H), 1.44 (d, *J* = 6.5 Hz, 3H); ¹³C NMR (101 MHz, CDCl₃) δ 158.8, 138.3, 126.7, 113.8, 69.6, 55.2, 25.1; 74% ee, HPLC Daicel column OD-H, 98% hexanes, 2% ^tPrOH, 1.0 mL/min, 11.1 min (major), 13.4 min (minor); HRMS (ESI-MS) *m/z* [M + Na]⁺ calcd for C₉H₁₂O₂Na 175.0730, found 175.0729.

(R)-1-(2-Chlorophenyl)ethan-1-ol (7e):¹⁷ colorless oil, 44.3 mg, yield 96%; [α]_D²⁰ = +32.55 (*c* = 0.19 in CHCl₃); ¹H NMR (400 MHz, CDCl₃) δ 7.58 (d, *J* = 7.7 Hz, 1H), 7.29 (d, *J* = 14.0 Hz, 2H), 7.20 (d, *J* = 5.9 Hz, 1H), 5.27 (s, 1H), 2.19 (s, 1H), 1.48 (d, *J* = 6.4 Hz, 3H); ¹³C NMR (101 MHz, CDCl₃) δ 143.1, 131.6, 129.4, 128.4, 127.2, 126.4, 67.0, 23.5; 81% ee, HPLC Daicel column IE, 98% hexanes, 2% ^tPrOH, 1.0 mL/min, 9.8 min (major), 13.1 min (minor); HRMS (ESI-MS) *m/z* [M + Na]⁺ calcd for C₈H₉ClONa 179.0234, found 179.0233, isotopic peak C₈H₉³⁷ClONa found 181.0245.

(*R*)-1-(3-Chlorophenyl)ethan-1-ol (**7f**):¹⁷ colorless oil, 44.8 mg, yield 97%; $[\alpha]_D^{20} = +47.45$ ($c = 0.22$ in CHCl_3); $^1\text{H NMR}$ (400 MHz, CDCl_3) δ 7.37 (s, 1H), 7.25 (d, $J = 5.5$ Hz, 3H), 4.87 (q, $J = 6.4$ Hz, 1H), 1.89 (s, 1H), 1.48 (d, $J = 6.5$ Hz, 3H); $^{13}\text{C NMR}$ (101 MHz, CDCl_3) δ 147.9, 134.4, 129.8, 127.5, 125.6, 123.5, 69.8, 25.3; 70% ee, HPLC Daicel column IE, 99% hexanes, 1% $^i\text{PrOH}$, 1.0 mL/min, 17.3 min (minor), 21.1 min (major); HRMS (ESI-MS) m/z $[\text{M} + \text{Na}]^+$ calcd for $\text{C}_8\text{H}_9\text{ClONa}$ 179.0234, found 179.0230, isotopic peak $\text{C}_8\text{H}_9^{37}\text{ClONa}$ found 181.0256.

(*R*)-1-(4-Chlorophenyl)ethan-1-ol (**7g**):¹⁷ colorless oil, 43.9 mg, yield 95%; $[\alpha]_D^{20} = +40.28$ ($c = 0.24$ in CHCl_3); $^1\text{H NMR}$ (400 MHz, CDCl_3) δ 7.31 (s, 4H), 4.88 (q, $J = 6.5$ Hz, 1H), 1.76 (s, 1H), 1.47 (d, $J = 6.5$ Hz, 3H); $^{13}\text{C NMR}$ (101 MHz, CDCl_3) δ 144.3, 130.9, 127.8, 126.8, 69.8, 25.3; 68% ee, HPLC Daicel column IE, 99% hexanes, 1% $^i\text{PrOH}$, 1.0 mL/min, 15.7 min (minor), 18.3 min (major); HRMS (ESI-MS) m/z $[\text{M} + \text{Na}]^+$ calcd for $\text{C}_8\text{H}_9\text{ClONa}$ 179.0234, found 179.0234, isotopic peak $\text{C}_8\text{H}_9^{37}\text{ClONa}$ found 181.0245.

(*R*)-1-(4-(Trifluoromethyl)phenyl)ethan-1-ol (**7h**):¹⁷ colorless oil, 55.9 mg, yield 98%; $[\alpha]_D^{20} = +31.84$ ($c = 0.18$ in CHCl_3); $^1\text{H NMR}$ (400 MHz, CDCl_3) δ 7.60 (d, $J = 8.1$ Hz, 2H), 7.48 (d, $J = 8.1$ Hz, 2H), 4.95 (q, $J = 6.5$ Hz, 1H), 2.03 (s, 1H), 1.50 (d, $J = 6.5$ Hz, 3H); $^{13}\text{C NMR}$ (101 MHz, CDCl_3) δ 149.7, 129.5 (q, $J = 32.4$ Hz), 125.6, 125.4 (q, $J = 3.6$ Hz), 124.2 (q, $J = 271.9$ Hz), 69.7, 25.2; $^{19}\text{F NMR}$ (377 MHz, CDCl_3) δ -62.47; 65% ee, HPLC Daicel column OD-H, 99% hexanes, 1% $^i\text{PrOH}$, 1.0 mL/min, 16.0 min (minor), 17.4 min (major); HRMS (ESI-MS) m/z $[\text{M} + \text{Na}]^+$ calcd for $\text{C}_9\text{H}_9\text{F}_3\text{ONa}$ 213.0498, found 213.0503.

(*R*)-1-Phenylpropan-1-ol (**7i**):²² colorless oil, 40.4 mg, yield 99%; $[\alpha]_D^{20} = +32.4$ ($c = 0.20$ in CHCl_3); $^1\text{H NMR}$ (400 MHz, CDCl_3) δ 7.40–7.35 (m, 4H), 7.34–7.29 (m, 1H), 4.62 (t, $J = 6.6$ Hz, 1H), 1.97 (s, 1H), 1.90–1.72 (m, 2H), 0.94 (t, $J = 7.4$ Hz, 3H); $^{13}\text{C NMR}$ (101 MHz, CDCl_3) δ 144.6, 128.4, 127.5, 126.0, 76.1, 31.9, 10.2; 71% ee, HPLC Daicel column OD-H, 98% hexanes, 2% $^i\text{PrOH}$, 1.0 mL/min, 13.5 min (major), 14.6 min (minor); HRMS (ESI-MS) m/z $[\text{M} + \text{Na}]^+$ calcd for $\text{C}_9\text{H}_{12}\text{ONa}$ 159.0780, found 159.0773.

Characteristic Data of Allylic Alcohols 9. (*R,E*)-1,3-Diphenylprop-2-en-1-ol (**9a**):⁸ colorless oil, 62.4 mg, yield 99%; $[\alpha]_D^{20} = +17.84$ ($c = 0.38$ in CHCl_3); $^1\text{H NMR}$ (400 MHz, CDCl_3) δ 7.42 (d, $J = 7.2$ Hz, 2H), 7.36 (t, $J = 7.9$ Hz, 4H), 7.33–7.25 (m, 3H), 7.25–7.19 (m, 1H), 6.67 (d, $J = 15.8$ Hz, 1H), 6.37 (dd, $J = 15.8, 6.5$ Hz, 1H), 5.36 (d, $J = 6.3$ Hz, 1H), 2.18 (s, 1H); $^{13}\text{C NMR}$ (101 MHz, CDCl_3) δ 142.8, 136.6, 131.6, 130.6, 128.6, 127.8, 126.7, 126.4, 75.2; 70% ee, HPLC Daicel column OD-H, 90% hexanes, 10% $^i\text{PrOH}$, 1.0 mL/min, 13.9 min (minor), 17.4 min (major); HRMS (ESI-MS) m/z $[\text{M} + \text{Na}]^+$ calcd for $\text{C}_{15}\text{H}_{14}\text{ONa}$ 233.0937, found 233.0937.

(*R,E*)-3-(3-Bromophenyl)-1-phenylprop-2-en-1-ol (**9b**): colorless oil, 83.0 mg, yield 97%; $[\alpha]_D^{20} = +10.25$ ($c = 0.26$ in CHCl_3); $^1\text{H NMR}$ (400 MHz, CDCl_3) δ 7.56 (s, 1H), 7.49–7.28 (m, 7H), 7.19 (t, $J = 7.8$ Hz, 1H), 6.65 (d, $J = 15.8$ Hz, 1H), 6.41 (dd, $J = 15.8, 6.2$ Hz, 1H), 5.40 (d, $J = 6.0$ Hz, 1H), 2.22 (s, 1H); $^{13}\text{C NMR}$ (101 MHz, CDCl_3) δ 142.5, 138.8, 133.1, 130.61, 130.1, 129.5, 128.8, 128.0, 126.4, 125.3, 122.8, 74.9; 50% ee, HPLC Daicel column IB, 95% hexanes, 5% $^i\text{PrOH}$, 1.0 mL/min, 14.1 min (minor), 20.5 min (major); HRMS (ESI-MS) m/z $[\text{M} + \text{Na}]^+$ calcd for $\text{C}_{15}\text{H}_{13}\text{BrONa}$ 311.0042, found 311.0044, isotopic peak $\text{C}_{15}\text{H}_{13}^{81}\text{BrONa}$ found 312.9964.

(*R,E*)-3-(3-Methoxyphenyl)-1-phenylprop-2-en-1-ol (**9c**): colorless oil, 71.3 mg, yield 99%; $[\alpha]_D^{20} = +12.37$ ($c = 0.30$ in CHCl_3); $^1\text{H NMR}$ (400 MHz, CDCl_3) δ 7.41 (d, $J = 7.2$ Hz, 2H), 7.35 (t, $J = 7.4$ Hz, 2H), 7.29 (d, $J = 7.1$ Hz, 1H), 7.20 (t, $J = 8.1$ Hz, 1H), 6.96 (d, $J = 7.7$ Hz, 1H), 6.90 (s, 1H), 6.78 (dd, $J = 8.1, 2.2$ Hz, 1H), 6.63 (d, $J = 15.8$ Hz, 1H), 6.35 (dd, $J = 15.8, 6.5$ Hz, 1H), 5.34 (d, $J = 6.4$ Hz, 1H), 3.77 (s, 3H), 2.32 (s, 1H); $^{13}\text{C NMR}$ (101 MHz, CDCl_3) δ 159.8, 142.8, 138.0, 131.9, 130.4, 129.6, 128.7, 127.8, 126.4, 119.4, 113.6, 111.9, 75.1, 55.3; 68% ee, HPLC Daicel column IB, 90% hexanes, 10% $^i\text{PrOH}$, 1.0 mL/min, 13.4 min (minor), 23.8 min (major); HRMS (ESI-MS) m/z $[\text{M} + \text{Na}]^+$ calcd for $\text{C}_{16}\text{H}_{16}\text{O}_2\text{Na}$ 263.1043, found 263.1041.

(*R,E*)-3-(4-Bromophenyl)-1-phenylprop-2-en-1-ol (**9d**): colorless oil, 81.2 mg, yield 95%; $[\alpha]_D^{20} = +9.84$ ($c = 0.32$ in CHCl_3); $^1\text{H NMR}$ (400 MHz, CDCl_3) δ 7.44–7.26 (m, 7H), 7.22 (t, $J = 7.0$ Hz, 2H), 6.59 (d, $J = 15.9$ Hz, 1H), 6.34 (dd, $J = 15.8, 6.3$ Hz, 1H), 5.33 (d, $J = 6.1$ Hz, 1H), 2.26 (s, 1H); $^{13}\text{C NMR}$ (101 MHz, CDCl_3) δ 142.6, 135.5, 132.3, 131.7, 129.2, 128.7, 128.1, 126.4, 121.6, 75.0; 61% ee, HPLC Daicel column IB, 95% hexanes, 5% $^i\text{PrOH}$, 1.0 mL/min, 12.4 min (major), 15.3 min (minor); HRMS (ESI-MS) m/z $[\text{M} + \text{Na}]^+$ calcd for $\text{C}_{15}\text{H}_{13}\text{BrONa}$ 311.0042, found 311.0041, isotopic peak $\text{C}_{15}\text{H}_{13}^{81}\text{BrONa}$ found 312.9976.

(*R,E*)-3-(4-Fluorophenyl)-1-phenylprop-2-en-1-ol (**9e**):⁸ colorless oil, 65.0 mg, yield 96%; $[\alpha]_D^{20} = +10.29$ ($c = 0.28$ in CHCl_3); $^1\text{H NMR}$ (400 MHz, CDCl_3) δ 7.46–7.26 (m, 7H), 6.98 (t, $J = 8.6$ Hz, 2H), 6.63 (d, $J = 15.9$ Hz, 1H), 6.29 (dd, $J = 15.8, 6.5$ Hz, 1H), 5.35 (d, $J = 6.1$ Hz, 1H), 2.14 (s, 1H); $^{13}\text{C NMR}$ (101 MHz, CDCl_3) δ 162.4 (d, $J = 247.0$ Hz), 142.8, 132.7 (d, $J = 3.4$ Hz), 131.3, 131.3, 129.4, 128.7, 128.2 (d, $J = 8.0$ Hz), 127.9, 126.4, 115.5 (d, $J = 21.6$ Hz), 75.1; $^{19}\text{F NMR}$ (377 MHz, CDCl_3) δ -114.12; 72% ee, HPLC Daicel column IB, 95% hexanes, 5% $^i\text{PrOH}$, 1.0 mL/min, 11.3 min (major), 13.3 min (minor); HRMS (ESI-MS) m/z $[\text{M} + \text{Na}]^+$ calcd for $\text{C}_{15}\text{H}_{13}\text{FONa}$ 251.0843, found 251.0836.

(*R,E*)-1-Phenyl-3-(4-(trifluoromethyl)phenyl)prop-2-en-1-ol (**9f**): colorless oil, 75.9 mg, yield 92%; $[\alpha]_D^{20} = +11.32$ ($c = 0.39$ in CHCl_3); $^1\text{H NMR}$ (400 MHz, CDCl_3) δ 7.54 (d, $J = 8.3$ Hz, 2H), 7.49–7.35 (m, 6H), 7.34–7.28 (m, 1H), 6.72 (d, $J = 15.9$ Hz, 1H), 6.47 (dd, $J = 15.9, 6.1$ Hz, 1H), 5.39 (d, $J = 5.8$ Hz, 1H), 2.22 (s, 1H); $^{13}\text{C NMR}$ (101 MHz, CDCl_3) δ 142.4, 140.1, 134.1, 129.6 (d, $J = 32.5$ Hz), 128.9, 128.8, 128.1, 126.8, 126.4, 125.5 (d, $J = 3.7$ Hz), 74.9; $^{19}\text{F NMR}$ (377 MHz, CDCl_3) δ -62.50; 80% ee, HPLC Daicel column IB, 90% hexanes, 10% $^i\text{PrOH}$, 1.0 mL/min, 6.9 min (major), 7.4 min (minor); HRMS (ESI-MS) m/z $[\text{M} + \text{Na}]^+$ calcd for $\text{C}_{16}\text{H}_{13}\text{F}_3\text{ONa}$ 301.0811, found 301.0809.

(*R,E*)-3-(4-Nitrophenyl)-1-phenylprop-2-en-1-ol (**9g**):⁸ colorless oil, 72.0 mg, yield 95%; $[\alpha]_D^{20} = +32.44$ ($c = 0.35$ in CHCl_3); $^1\text{H NMR}$ (400 MHz, CDCl_3) δ 8.08 (d, $J = 8.6$ Hz, 2H), 7.42 (d, $J = 8.7$ Hz, 2H), 7.33 (q, $J = 8.1$ Hz, 4H), 7.26 (d, $J = 6.7$ Hz, 1H), 6.70 (d, $J = 15.9$ Hz, 1H), 6.48 (dd, $J = 15.9, 5.8$ Hz, 1H), 5.35 (d, $J = 5.7$ Hz, 1H), 2.18 (s, 1H); $^{13}\text{C NMR}$ (101 MHz, CDCl_3) δ 143.2, 142.1, 136.3, 128.9, 128.3, 127.9, 127.1, 126.4, 124.0, 74.7; 75% ee, HPLC Daicel column OD-H, 90% hexanes, 10% $^i\text{PrOH}$, 1.0 mL/min, 21.8 min (major), 23.4 min (minor); HRMS (ESI-MS) m/z $[\text{M} + \text{Na}]^+$ calcd for $\text{C}_{15}\text{H}_{13}\text{NO}_3\text{Na}$ 278.0788, found 278.0784.

(*R,E*)-1-Phenyl-3-(*p*-tolyl)prop-2-en-1-ol (**9h**):⁸ colorless oil, 64.6 mg, yield 97%; $[\alpha]_D^{20} = +18.85$ ($c = 0.42$ in CHCl_3); $^1\text{H NMR}$ (400 MHz, CDCl_3) δ 7.48 (d, $J = 7.3$ Hz, 2H), 7.42 (t, $J = 7.4$ Hz, 2H), 7.34 (t, $J = 8.0$ Hz, 3H), 7.17 (d, $J = 7.9$ Hz, 2H), 6.69 (d, $J = 15.8$ Hz, 1H), 6.38 (dd, $J = 15.8, 6.6$ Hz, 1H), 5.40 (d, $J = 6.6$ Hz, 1H), 2.39 (s, 3H), 2.26 (s, 1H); $^{13}\text{C NMR}$ (101 MHz, CDCl_3) δ 143.0, 137.7, 133.8, 130.6, 129.3, 128.6, 127.8, 126.5, 75.2, 21.3; 67% ee, HPLC Daicel column IB, 95% hexanes, 5% $^i\text{PrOH}$, 1.0 mL/min, 12.0 min (major), 15.2 min (minor); HRMS (ESI-MS) m/z $[\text{M} + \text{Na}]^+$ calcd for $\text{C}_{16}\text{H}_{16}\text{ONa}$ 247.1093, found 247.1094.

(*R,E*)-3-(4-(*tert*-Butyl)phenyl)-1-phenylprop-2-en-1-ol (**9i**):⁸ colorless oil, 79.1 mg, yield 99%; $[\alpha]_D^{20} = +15.74$ ($c = 0.42$ in CHCl_3); $^1\text{H NMR}$ (400 MHz, CDCl_3) δ 7.42–7.23 (m, 9H), 6.63 (d, $J = 15.8$ Hz, 1H), 6.31 (dd, $J = 15.8, 6.6$ Hz, 1H), 5.31 (d, $J = 4.4$ Hz, 1H), 2.34 (d, $J = 3.1$ Hz, 1H), 1.29 (s, 9H); $^{13}\text{C NMR}$ (101 MHz, CDCl_3) δ 156.0, 143.0, 133.8, 130.9, 130.4, 128.6, 127.8, 126.4, 125.6, 75.2, 34.7, 31.4; 50% ee, HPLC Daicel column IB, 98% hexanes, 2% $^i\text{PrOH}$, 1.0 mL/min, 17.4 min (major), 18.4 min (minor); HRMS (ESI-MS) m/z $[\text{M} + \text{Na}]^+$ calcd for $\text{C}_{19}\text{H}_{22}\text{ONa}$ 289.1563, found 289.1564.

(*R,E*)-3-(Naphthalen-2-yl)-1-phenylprop-2-en-1-ol (**9j**): colorless oil, 76.4 mg, yield 98%; $[\alpha]_D^{20} = +23.52$ ($c = 0.45$ in CHCl_3); $^1\text{H NMR}$ (400 MHz, CDCl_3) δ 7.79–7.68 (m, 4H), 7.59–7.52 (m, 1H), 7.48–7.39 (m, 4H), 7.37 (t, $J = 7.7$ Hz, 2H), 7.29 (t, $J = 7.2$ Hz, 1H), 6.80 (d, $J = 15.8$ Hz, 1H), 6.48 (dd, $J = 15.8, 6.5$ Hz, 1H), 5.39 (d, $J = 6.4$ Hz, 1H), 2.28 (s, 1H); $^{13}\text{C NMR}$ (101 MHz, CDCl_3) δ 142.7, 134.1, 133.6, 133.1, 132.0, 130.7, 128.7, 128.3, 127.9, 126.8, 126.4, 126.0, 123.7, 75.2; 62% ee, HPLC Daicel column IB, 90% hexanes, 10% $^i\text{PrOH}$, 1.0 mL/min, 11.0 min (major), 12.2 min (minor);

HRMS (ESI-MS) m/z $[M + Na]^+$ calcd for $C_{19}H_{16}ONa$ 283.1093, found 283.1100.

(*R,E*)-1-(4-Fluorophenyl)-3-phenylprop-2-en-1-ol (**9k**): colorless oil, 67.1 mg, yield 98%; $[\alpha]_D^{20} = +8.84$ ($c = 0.48$ in $CHCl_3$); 1H NMR (400 MHz, $CDCl_3$) δ 7.38 (dd, $J = 8.1, 6.2$ Hz, 4H), 7.30 (t, $J = 7.5$ Hz, 2H), 7.24 (d, $J = 7.0$ Hz, 1H), 7.03 (t, $J = 8.6$ Hz, 2H), 6.65 (d, $J = 15.9$ Hz, 1H), 6.33 (dd, $J = 15.8, 6.5$ Hz, 1H), 5.34 (d, $J = 6.5$ Hz, 1H), 2.21 (s, 1H); ^{13}C NMR (101 MHz, $CDCl_3$) δ 162.4 (d, $J = 245.8$ Hz), 138.5 (d, $J = 3.1$ Hz), 136.4, 131.3, 130.8, 128.7, 128.1 (d, $J = 8.1$ Hz), 128.0, 126.7, 115.5 (d, $J = 21.6$ Hz), 74.5. ^{19}F NMR (377 MHz, $CDCl_3$) δ -114.7; 48% ee, HPLC Daicel column IB, 90% hexanes, 10% iPrOH , 1.0 mL/min, 6.9 min (minor), 7.4 min (major); HRMS (ESI-MS) m/z $[M + Na]^+$ calcd for $C_{15}H_{13}FONa$ 251.0843, found 251.0838.

(*R,E*)-1-(4-Methoxyphenyl)-3-phenylprop-2-en-1-ol (**9l**): colorless oil, 71.3 mg, yield 99%; $[\alpha]_D^{20} = +7.49$ ($c = 0.33$ in $CHCl_3$); 1H NMR (400 MHz, $CDCl_3$) δ 7.45 (d, $J = 7.5$ Hz, 2H), 7.41–7.36 (m, 4H), 7.26 (t, $J = 8.6$ Hz, 3H), 6.73 (d, $J = 15.9$ Hz, 1H), 6.49–6.40 (m, 1H), 5.40 (d, $J = 6.4$ Hz, 1H), 2.43 (d, $J = 4.0$ Hz, 3H); ^{13}C NMR (101 MHz, $CDCl_3$) δ 140.0, 137.5, 136.7, 131.8, 130.3, 129.4, 128.6, 127.8, 126.7, 126.4, 77.5, 77.2, 76.9, 75.0, 21.2; 50% ee, HPLC Daicel column IB, 95% hexanes, 5% iPrOH , 1.0 mL/min, 6.9 min (minor), 7.4 min (major). HRMS (ESI-MS) m/z $[M + Na]^+$ calcd for $C_{16}H_{16}O_2Na$ 263.1043, found 263.1041.

■ ASSOCIATED CONTENT

Supporting Information

The Supporting Information is available free of charge at <https://pubs.acs.org/doi/10.1021/acs.organomet.1c00272>.

Experimental procedures, characterization data, HPLC chromatograms, and X-ray data for complexes 1–5 (PDF)

Accession Codes

CCDC 2050142, 2050145, 2050150, 2051400, 2054260, 2055968, and 2081007 contain the supplementary crystallographic data for this paper. These data can be obtained free of charge via www.ccdc.cam.ac.uk/data_request/cif, or by emailing data_request@ccdc.cam.ac.uk, or by contacting The Cambridge Crystallographic Data Centre, 12 Union Road, Cambridge CB2 1EZ, UK; fax: +44 1223 336033.

■ AUTHOR INFORMATION

Corresponding Authors

Chengrong Lu – College of Chemistry, Chemical Engineering and Materials Science, Key Laboratory of Organic Synthesis of Jiangsu Province, Dushu Lake Campus, Soochow University, Suzhou 215123, People's Republic of China; Email: luchengrong@suda.edu.cn

Bei Zhao – College of Chemistry, Chemical Engineering and Materials Science, Key Laboratory of Organic Synthesis of Jiangsu Province, Dushu Lake Campus, Soochow University, Suzhou 215123, People's Republic of China; orcid.org/0000-0001-8687-2632; Email: zhaobei@suda.edu.cn

Author

Qishun Yu – College of Chemistry, Chemical Engineering and Materials Science, Key Laboratory of Organic Synthesis of Jiangsu Province, Dushu Lake Campus, Soochow University, Suzhou 215123, People's Republic of China

Complete contact information is available at: <https://pubs.acs.org/doi/10.1021/acs.organomet.1c00272>

Notes

The authors declare no competing financial interest.

■ ACKNOWLEDGMENTS

We gratefully acknowledge financial support from the National Natural Science Foundation of China (Grant No. 21572151), the Natural Science Foundation of the Jiangsu Higher Education Institutions of China (Grant No. 19KJA320007), the project of scientific and technological infrastructure of Suzhou (SZS201708), and the PAPD.

■ REFERENCES

- (1) (a) Fujii, A.; Hashiguchi, A.; Uematsu, N.; et al. Ruthenium(II)-Catalyzed Asymmetric Transfer Hydrogenation of Ketones Using a Formic Acid-Triethylamine Mixture. *J. Am. Chem. Soc.* **1996**, *118*, 2521–2522. (b) Matharu, D. S.; Morris, D. J.; Kawamoto, A. M.; Clarkson, G. J.; Wills, M. A Stereochemically Well-Defined Rhodium(III) Catalyst for Asymmetric Transfer Hydrogenation of Ketones. *Org. Lett.* **2005**, *7*, 5489–5491. (c) Martins, J. E. D.; Clarkson, G. J.; Wills, M. Ru(II) Complexes of *N*-Alkylated TsDPEN Ligands in Asymmetric Transfer Hydrogenation of Ketones and Imines. *Org. Lett.* **2009**, *11*, 847–850. (d) Soni, R.; Hall, T. H.; Morris, D. J.; Clarkson, G. J.; Owen, M. R.; Wills, M. *N*-Functionalised TsDPEN Catalysts for Asymmetric Transfer Hydrogenation; Synthesis and Applications. *Tetrahedron Lett.* **2015**, *56*, 6397–6401.
- (2) (a) Watanabe, M.; Murata, K.; Ikariya, T. Enantioselective Michael Reaction Catalyzed by Well-Defined Chiral Ru Amido Complexes: Isolation and Characterization of the Catalyst Intermediate, Ru Malonate Complex Having a Metal–Carbon Bond. *J. Am. Chem. Soc.* **2003**, *125*, 7508–7509. (b) Chen, G.; Liang, G.; Wang, Y.; Deng, P.; Zhou, H. A Homodinuclear Cobalt Complex for the Catalytic Asymmetric Michael Reaction of β -Ketoesters to Nitroolefins. *Org. Biomol. Chem.* **2018**, *16*, 3841–3850.
- (3) Zhang, S.; Deng, P.; Zhou, J.; Liu, M.; Liang, G.; Xiong, Y.; Zhou, H. A Novel Homobimetallic Nickel Complex for the Asymmetric Direct Mannich Reaction of Imines: A Practical Method on a Multi-Gram Scale. *Chem. Commun.* **2017**, *53*, 12914–12917.
- (4) (a) Gelalcha, F. G.; Bitterlich, B.; Anilkumar, G.; Tse, M. K.; Beller, M. Iron-Catalyzed Asymmetric Epoxidation of Aromatic Alkenes Using Hydrogen Peroxide. *Angew. Chem., Int. Ed.* **2007**, *46*, 7293–7296. (b) Gelalcha, F. G.; Anilkumar, G.; Tse, M. K.; Brückner, A.; Beller, M. Biomimetic Iron-Catalyzed Asymmetric Epoxidation of Aromatic Alkenes by Using Hydrogen Peroxide. *Chem. - Eur. J.* **2008**, *14*, 7687–7698. (c) Malkov, A. V.; Czerny, L.; Malyshev, D. A. Vanadium-Catalyzed Asymmetric Epoxidation of Allylic Alcohols in Water. *J. Org. Chem.* **2009**, *74*, 3350–3355.
- (5) Chen, Q.-G.; Tang, Y.; Huang, T.-Y.; Liu, X.-H.; Lin, L.-L.; Feng, X.-M. Copper/Guanidine-Catalyzed Asymmetric Alkynylation of Isatins. *Angew. Chem., Int. Ed.* **2016**, *55*, 5286–5289.
- (6) Qian, Q.-Q.; Zhu, W.-G.; Lu, C.-R.; Zhao, B.; Yao, Y.-M. Asymmetric Michael Addition of Malonates to Unsaturated Ketones Catalyzed by Rare Earth Metal Complexes Bearing Phenoxy Functionalized Chiral Diphenylprolinolate Ligands. *Tetrahedron: Asymmetry* **2016**, *27*, 911–917.
- (7) (a) Qian, Q.-Q.; Tan, Y.-F.; Zhao, B.; Feng, T.; Shen, Q.; Yao, Y.-M. Asymmetric Epoxidation of Unsaturated Ketones Catalyzed by Heterobimetallic Rare Earth–Lithium Complexes Bearing Phenoxy-Functionalized Chiral Diphenylprolinolate Ligand. *Org. Lett.* **2014**, *16*, 4516–4519. (b) Zeng, C.; Yuan, D.; Zhao, B.; Yao, Y.-M. Highly Enantioselective Epoxidation of α,β -Unsaturated Ketones Catalyzed by Rare-Earth Amides $[(Me_3Si)_2N]_3RE(\mu-Cl)Li(THF)_3$ with Phenoxy-Functionalized Chiral Prolinols. *Org. Lett.* **2015**, *17*, 2242–2245.
- (8) Song, P.; Lu, C.-R.; Fei, Z.-H.; Zhao, B.; Yao, Y.-M. Enantioselective Reduction of Ketones Catalyzed by Rare-Earth Metals Complexed with Phenoxy Modified Chiral Prolinols. *J. Org. Chem.* **2018**, *83*, 6093–6100.
- (9) Fei, Z.-H.; Zeng, C.; Lu, C.-R.; Zhao, B.; Yao, Y.-M. An Efficient Asymmetric Hydrophosphonylation of Unsaturated Amides Catalyzed by Rare-Earth Metal Amides $[(Me_3Si)_2N]_3RE(\mu-Cl)Li(THF)_3$ with Phenoxy-Functionalized Chiral Prolinols. *RSC Adv.* **2017**, *7*, 19306–19311.

(10) Kubota, K.; Hamblett, C. L.; Wang, X.; Leighton, J. L. Strained Silacycle-Catalyzed Asymmetric Diels-Alder Cycloadditions: the First Highly Enantioselective Silicon Lewis Acid Catalyst. *Tetrahedron* **2006**, *62*, 11397–11401.

(11) Guo, J.; Chen, J.-H.; Lu, Z. Cobalt-Catalyzed Asymmetric Hydroboration of Aryl Ketones with Pinacolborane. *Chem. Commun.* **2015**, *51*, 5725–5727.

(12) Vasilenko, V.; Blasius, C. K.; Wadepohl, H.; Gade, L. H. Mechanism-Based Enantiodivergence in Manganese Reduction Catalysis: A Chiral Pincer Complex for the Highly Enantioselective Hydroboration of Ketones. *Angew. Chem., Int. Ed.* **2017**, *56*, 8393–8397.

(13) Chen, F.-L.; Zhang, Y.; Yu, L.; Zhu, S.-L. Enantioselective NiH/Pmrox-Catalyzed 1,2-Reduction of α,β -Unsaturated Ketones. *Angew. Chem., Int. Ed.* **2017**, *56*, 2022–2025.

(14) Falconnet, A.; Magre, M.; Maity, B.; Cavallo, L.; Rueping, M. Asymmetric Magnesium-Catalyzed Hydroboration by Metal-Ligand Cooperative Catalysis. *Angew. Chem., Int. Ed.* **2019**, *58*, 17567–17571.

(15) Lebedev, Y.; Polishchuk, I.; Maity, B.; Dinis Veloso Guerreiro, M.; Cavallo, L.; Rueping, M. Asymmetric Hydroboration of Heteroaryl Ketones by Aluminum Catalysis. *J. Am. Chem. Soc.* **2019**, *141*, 19415–19423.

(16) He, P.; Liu, X.-H.; Zheng, H.-F.; Li, W.; Lin, L.-L.; Feng, X.-M. Asymmetric 1,2-Reduction of Enones with Potassium Borohydride Catalyzed by Chiral N,N' -Dioxide-Scandium(III) Complexes. *Org. Lett.* **2012**, *14*, 5134–5137.

(17) Sun, Y.-L.; Lu, C.-R.; Zhao, B.; Xue, M.-Q. Enantioselective Hydroboration of Ketones Catalyzed by Rare-Earth Metal Complexes Containing Trost Ligands. *J. Org. Chem.* **2020**, *85*, 10504–10513.

(18) (a) Farina, V.; Reeves, J. T.; Senanayake, C. H.; Song, J. J. Asymmetric Synthesis of Active Pharmaceutical Ingredients. *Chem. Rev.* **2006**, *106*, 2734–2793. (b) Li, Y.-Y.; Yu, S.-L.; Shen, W.-Y.; Gao, J.-X. Iron-, Cobalt-, and Nickel-Catalyzed Asymmetric Transfer Hydrogenation and Asymmetric Hydrogenation of Ketones. *Acc. Chem. Res.* **2015**, *48*, 2587–2598. (c) Klingler, F. D. Asymmetric Hydrogenation of Prochiral Amino Ketones to Amino Alcohols for Pharmaceutical Use. *Acc. Chem. Res.* **2007**, *40*, 1367–1376. (d) Liu, H.; de Souza, F. Z. R.; Liu, L.; Chen, B.-S. The Use of Marine-Derived Fungi for Preparation of Enantiomerically Pure Alcohols. *Appl. Microbiol. Biotechnol.* **2018**, *102*, 1317–1330.

(19) Balsells, J.; Meorado, L.; Phillips, M.; Ortega, F.; Aguirre, G.; Somanathan, R.; Walsh, P. J. Synthesis of Chiral Sulfonamide/Schiff Base Ligands. *Tetrahedron: Asymmetry* **1998**, *9*, 4135–4142.

(20) Weekes, D. M.; Diebold, C.; Mobian, P.; Huguenard, C.; Allouche, L.; Henry, M. A Remarkable Solvent Effect on the Nuclearity of Neutral Titanium (IV)-Based Helicate Assemblies. *Chem. - Eur. J.* **2014**, *20*, 5092–5101.

(21) Frisch, M. J.; Trucks, G. W.; Schlegel, H. B.; Scuseria, G. E., et al. *Gaussian16, Rev. B.01*; Gaussian, Inc.: Wallingford, CT, 2016.

(22) Ling, F.; Nian, S.; Chen, J.; Luo, W.; Wang, Z.; Lv, Y.; Zhong, W. Development of Ferrocene-Based Diamine-Phosphine-Sulfonamide Ligands for Iridium-Catalyzed Asymmetric Hydrogenation of Ketones. *J. Org. Chem.* **2018**, *83*, 10749–10761.